

Highly efficient reforming of toluene to syngas in a gliding arc plasma reactor

Danhua Mei¹, Peng Zhang¹, Shiyun Liu¹, Liang Ding¹, Yichen Ma², Renwu Zhou³, Haochi Gu¹, Zhi Fang^{1,*}, Patrick J. Cullen³, Xin Tu^{2,*}

1 College of Electrical Engineering and Control Science, Nanjing Tech University, Nanjing 211816, Jiangsu China

2 Department of Electrical Engineering and Electronics, University of Liverpool, Liverpool, L69 3GJ, UK

3 School of Chemical and Biomolecular Engineering, University of Sydney, NSW 2006, Australia

***Corresponding authors**

Prof. Xin Tu

Department of Electrical Engineering and Electronics,
University of Liverpool
Liverpool L69 3GJ
UK

Email: xin.tu@liverpool.ac.uk

Prof. Zhi Fang

College of Electrical Engineering and Control Science
Nanjing Tech University
Nanjing, Jiangsu 211816
China

E-mail: myfz@263.net

26 **Abstract**

27 Plasma reforming is a promising technology to transform tars from biomass gasification into
28 valuable fuels and chemicals. However, the key performance (tar conversion, gas yield and energy
29 efficiency) of the plasma tar reforming process can be significantly influenced by operating
30 conditions such as the gas composition. In this study, the effect of CO₂, steam and O₂ on the plasma
31 reforming of toluene, a model tar compound, was investigated in a gliding arc (GA) reactor.
32 Compared to the plasma reforming of toluene with N₂, the presence of oxidative gases (CO₂, H₂O
33 and O₂) can generate a highly reactive plasma environment, thus creating new reaction pathways in
34 the plasma conversion of toluene. The optimal content of CO₂, H₂O and O₂ to balance the toluene
35 conversion, syngas yield and energy efficiency in the plasma reforming was 2 vol.%, 4 vol.% and 2
36 vol.%, respectively, suggesting that the presence of an appropriate amount of oxidative gas (CO₂,
37 H₂O and O₂) is important to maximize the key performance of the plasma reforming process. The
38 highest toluene conversion of 78.3%, syngas yield of 73.9% and energy efficiency of 69.5 g/kWh
39 were achieved simultaneously in the plasma reforming of toluene containing 4 vol.% steam. The
40 proposed reaction pathways in the plasma reforming of toluene have been proposed through the
41 analysis of gas and liquid products coupled with optical emission spectroscopic diagnostics.

42

43 **Keywords:** Non-thermal plasma; gliding arc discharge; tar reforming; syngas; biomass gasification

44 **1. Introduction**

45 Biomass gasification is a promising technology that can effectively convert biomass into valuable
46 producer gas containing H₂, CO, CO₂ and CH₄. The contamination of producer gas with tars remains
47 a significant challenge in the gasification process [1], which may pose potential blockages and fouling
48 in downstream equipment, induce coke formation and reduce the overall heating value of producer
49 gas. These issues limit the efficiency of biomass gasification and bring threats to the safety of the
50 overall process. Tar is a mixture of condensable hydrocarbons with one or more benzene rings, and
51 its concentration in producer gas is dependent on the types and operational conditions of the gasifier,
52 varying from 1 to 100 g/Nm³. The carcinogenicity of tars has also been clearly demonstrated, which
53 can cause significant damage to the physical and mental health of human beings [2]. Therefore, cost-
54 effective removing tars from the gasified producer gas is critical in biomass gasification.

55 Non-thermal plasma technology provides an attractive and promising approach for the conversion
56 of tars into syngas at mild conditions. Non-thermal plasmas can produce highly energetic electrons
57 and a variety of reactive species (e.g., excited species and radicals), all of which can induce various
58 chemical reactions at relatively low temperatures [3-7]. Compared to thermal technologies, high
59 reaction rates and fast attainment of steady-state allow rapid start-up and shutdown of the plasma
60 process, which significantly reduces the overall energy costs [8-16]. The removal of tar model
61 compounds, including toluene, naphthalene and benzene, has been investigated using various plasma
62 discharges, such as corona discharge[17], pulsed spark discharge [18], dielectric barrier discharge
63 (DBD) [19-21] and gliding arc (GA) [22-29]. Compared with other types of plasma, GA has higher
64 electron densities (10^{23} - 10^{24} m⁻³) and can work efficiently in a wide range of gas flow rate and plasma
65 power [30]. These advantages make GA an attract and promising solution for highly efficient

66 conversion of tars to syngas.

67 From industrial applications point of view, the type of gasifying agents such as steam, air, oxygen
68 and their mixture, is one of the most important factors affecting the overall efficiency of biomass
69 gasification and the quality of producer gas [1]. The presence of oxygen in biomass gasification favors
70 the reduction of tars but might lead to the production of lower CO content in producer gas [29].
71 Generally, the producer gas from biomass gasification contains 10-13 vol.% CO₂ and ~10 vol.%
72 steam [31]. Therefore, understanding the influence of the gasifying agents on the plasma tar reforming
73 process is important to improve the efficiency of the plasma process. Therefore, it is critical to
74 investigate the plasma reforming of biomass tars using different working gases to better understand
75 the influence of the gasifying agents on the plasma tar conversion including the reaction pathways,
76 which can generate valuable information for the optimization of the plasma tar reforming process to
77 deliver clean and high-quality syngas.

78 In this work, a GA reactor was developed for plasma reforming of tars. Toluene was selected as the
79 tar model compound from biomass gasification . Pure nitrogen and a mixture of nitrogen and
80 oxidative gases (CO₂, H₂O and O₂) were used as the working gas individually. The effect of the
81 concentration of these oxidative gases on the performance of the plasma toluene reforming was
82 evaluated in terms of toluene conversion, syngas yield and energy efficiency. Optical emission
83 spectroscopic (OES) diagnostics was performed to understand the roles of reactive species in the
84 plasma reforming of toluene.

85

86 **2. Experimental**

87 **2.1 Experimental setup**

88 The plasma tar reforming experiments were carried out in a GA reactor (Figure 1) which consists
89 of two stainless steel knife-shaped electrodes (length: 60 mm; width: 18 mm; depth: 3 mm) and a gas
90 nozzle with an outlet diameter of 1.5 mm. The gas nozzle was fixed in the center of a ceramic plate,
91 while the electrodes were placed symmetrically on both sides of the gas nozzle with the narrowest
92 gap (electrode throat) of 2 mm. The distance between the electrode throat and the nozzle outlet was
93 5 mm. Gliding arc can be generated and maintained using an AC high voltage power source (10 kV/50
94 Hz). The arc voltage was measured using a Tektronix high voltage probe (P6015A) and the arc current
95 was sampled using a Magnelab Rogowski-coil current probe (CT-E 0.5-BNC). Both electrical signals
96 were recorded using a Tektronix digital oscilloscope (TDS2014B).

97 Different gas compositions (N_2 , CO_2/N_2 , $\text{H}_2\text{O}/\text{N}_2$ and O_2/N_2) were used in this study. A mixture
98 of toluene (99.5%, Sigma China) and carrier gas (N_2 , CO_2/N_2 , or O_2/N_2) was preheated at 180 °C in
99 a tube furnace before injecting into the GA reactor. In the plasma steam reforming of toluene, a
100 mixture of toluene (99.5%, Sigma China) and deionized water was carried by N_2 and preheated at
101 180 °C. The flow rate of toluene and deionized water was controlled independently with syringe
102 pumps (TYD01). The content of CO_2 , O_2 and steam was varied from 0 to 10 vol.%. The total flow
103 rate of the mixed gas stream flowing into the GA reactor was kept constant at 3.5 L/min, while the
104 initial concentration of toluene and the specific energy input (SEI) were 14.8 g/ Nm^3 and 0.17 kWh/ m^3 ,
105 respectively.

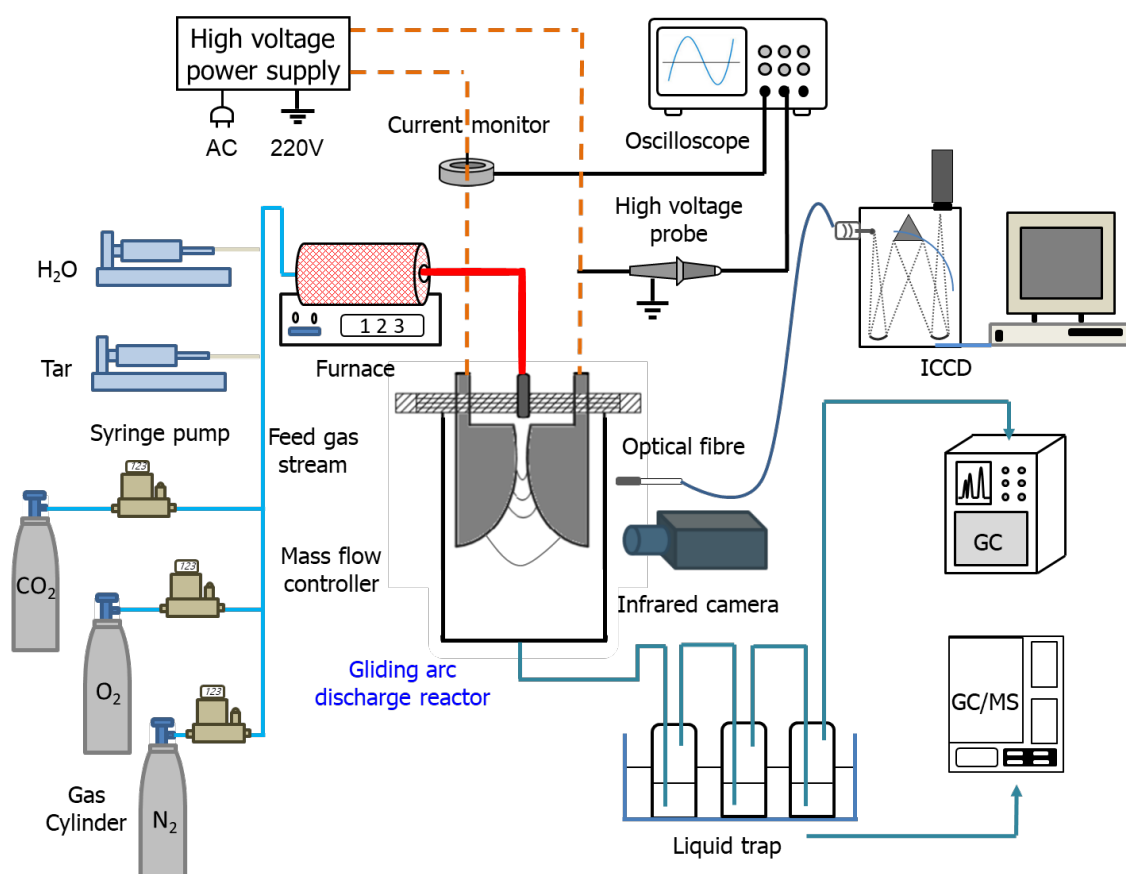
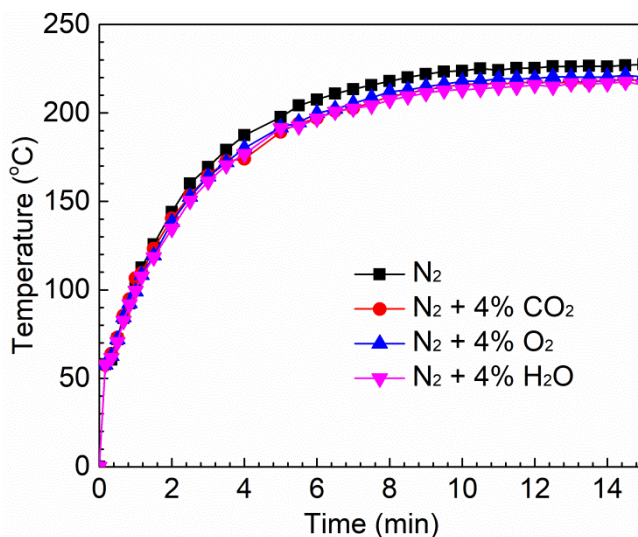


Figure 1. The scheme of the experimental setup.

2.2 Analytical methods

The produced gas stream passed through a cold trap containing three successive absorption bottles immersed in an ice and water mixture. Dichloromethane was contained in the first two bottles to absorb the condensable products, while the last bottle was kept empty to collect remaining entrained droplets. The gaseous products were collected at the exit of the cold trap using sampling bags and were analyzed using gas chromatography (Techcomp GC7900). The condensed by-products were qualitatively analyzed by gas chromatography-mass spectrometry (GC-MS, Agilent 7820A-5975C) using a standard library of the National Institute of Standards and Technology (NIST), while the concentration of unreacted toluene in the collected liquids was quantitatively determined by GC-MS through the calibration using a wide range of toluene concentration.

119 The emission spectra of the GA were recorded using an optical fiber connected to a Princeton
 120 Instrument ICCD spectrometer (Model-320-PI). The relative intensities of the selected molecular
 121 bands were determined using the relative peak intensity of the relevant band heads taken with the
 122 same settings of the spectrometer. The wall temperature of the GA reactor was measured using an
 123 infrared camera (Fotric 325Pro). The wall temperature of the GA reactor was almost constant (below
 124 230 °C) after switching on the plasma for 10 min at a total gas flow rate of 3.5 L/min and an SEI of
 125 0.17 kWh/m³ (Figure 2). The influence of different gas compositions on the wall temperature of the
 126 GA reactor was limited.



127
 128 Figure 2. The wall temperature of the GA reactor (total gas flow rate: 3.5 L/min; SEI: 0.17
 129 kWh/m³).

130 The discharge power was calculated as the time-averaged product of the arc voltage and arc
 131 current per cycle, while SEI was determined using Eq. (1).

$$132 \text{ SEI}(\text{kWh}/\text{m}^3) = \frac{P(\text{kW})}{\text{Total gas flow rate}(\text{m}^3/\text{h})} \quad (1)$$

133 The conversion of toluene and yield of major gas products were expressed as follows:

$$134 \quad X_{C_7H_8} (\%) = \frac{\text{toluene input (mol/s)} - \text{toluene output (mol/s)}}{\text{toluene input (mol/s)}} \times 100 \quad (2)$$

$$135 \quad Y_{H_2} (\%) = \frac{2 \times H_2 \text{ produced (mol/s)}}{8 \times C_7H_8 \text{ input (mol/s)} + 2 \times H_2O \text{ input (mol/s)}} \times 100 \quad (3)$$

$$136 \quad Y_{CO} (\%) = \frac{CO \text{ produced (mol/s)}}{7 \times C_7H_8 \text{ input (mol/s)} + CO_2 \text{ input (mol/s)}} \times 100 \quad (4)$$

$$137 \quad Y_{C_xH_y} (\%) = \frac{x \times C_xH_y \text{ produced (mol/s)}}{7 \times C_7H_8 \text{ input (mol/s)}} \times 100 \quad (5)$$

138 The carbon balance of the plasma process was determined by:

$$139 \quad B_{Carbon} (\%) = \frac{(7 \times C_7H_8)_{unconverted} \text{ (mol/s)} + x \times C_xH_y \text{ produced (mol/s)} + CO_{x \text{ produced}} \text{ (mol/s)}}{(7 \times C_7H_8)_{input} \text{ (mol/s)} + CO_2 \text{ input (mol/s)}} \times 100 \quad (6)$$

140 The energy efficiency of the plasma toluene conversion was calculated by:

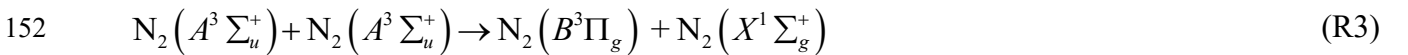
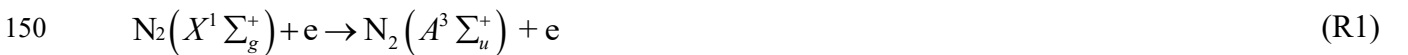
$$141 \quad \eta (\text{g/kWh}) = \frac{\text{Converted } C_7H_8 \text{ (g/m}^3\text{)}}{\text{SEI (kWh/m}^3\text{)}} \quad (7)$$

142

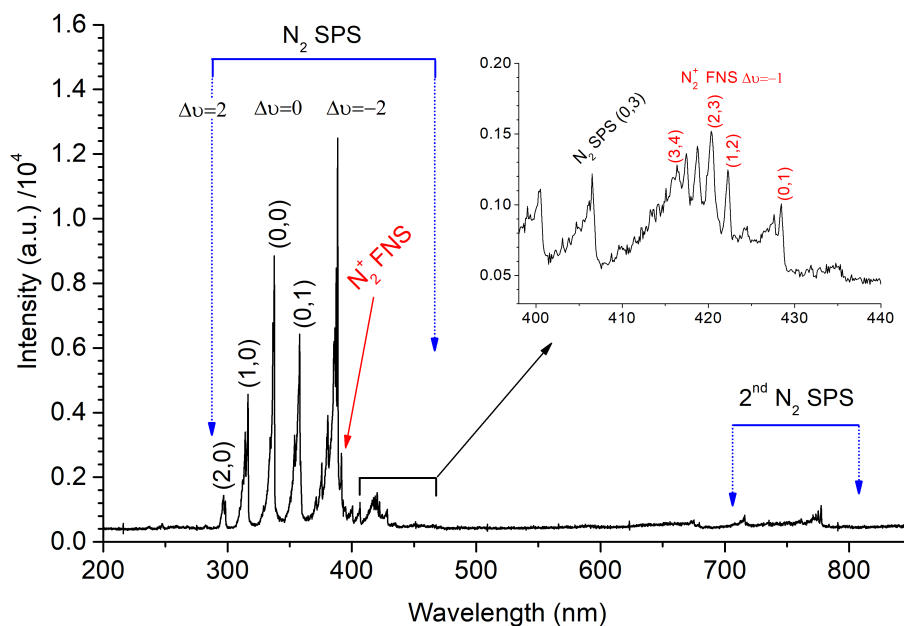
143 3. Results and discussion

144 3.1 Emission spectroscopic diagnostics

145 Figure 3 displays the emission spectra of the GA using different gas compositions. The spectrum
 146 of the pure nitrogen GA is dominated by the second positive system (SPS) of N_2 ($C^3\Pi_u \rightarrow B^3\Pi_g$)
 147 and the N_2^+ first negative system (FNS) ($B^2\Sigma_u^+ \rightarrow X^2\Sigma_g^+$) between 280 and 430 nm, suggesting the
 148 presence of nitrogen molecules at different excited states N_2^* , such as $N_2(A^3\Sigma_u^+)$, $N_2(B^3\Pi_g)$, $N_2(a')$
 149 and $N_2(C^3\Pi_u)$ via the reaction R1-R3.



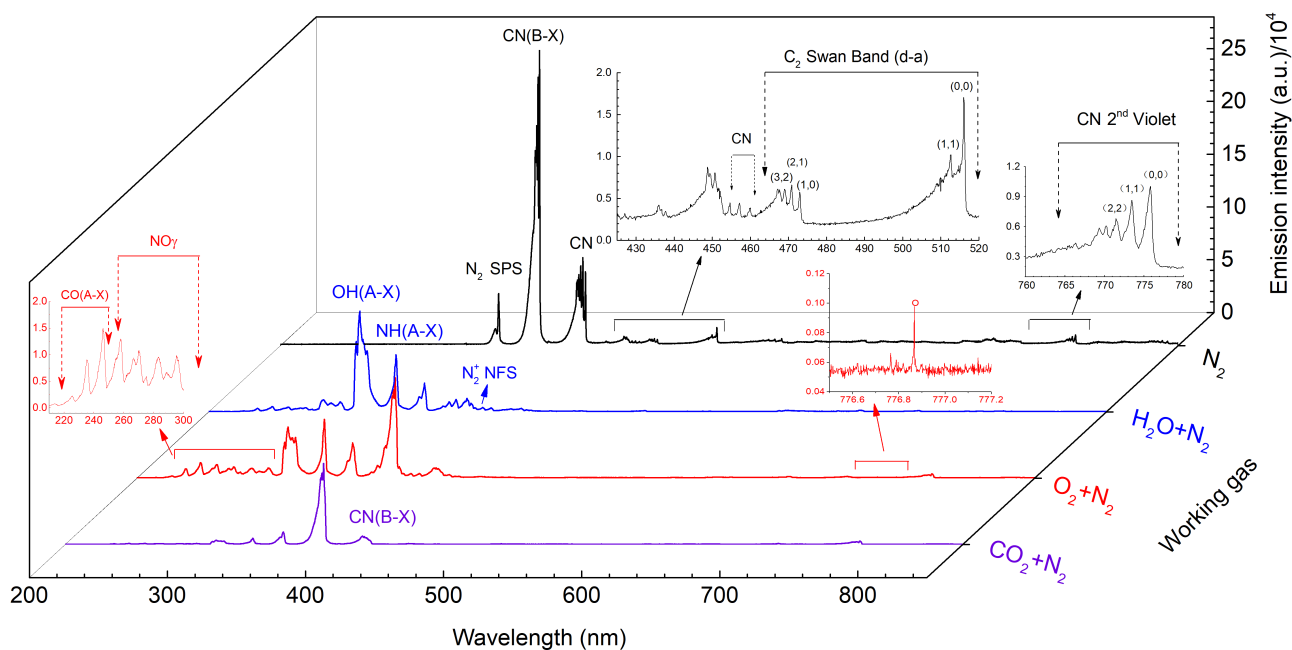
153



(a)

154

155



(b)

156

157

158 Figure 3. Optical emission spectra: (a) pure N_2 GA; (b) GA using different oxidative gases (CO_2

159 content: 4 vol.%, H_2O content 4 vol.%, O_2 content: 4 vol.%) (600 g/mm grating, exposure time 0.1

160

s).

161

162 The spectrum of the N₂/C₇H₈ GA is dominated by the CN ($B^2 \Sigma \rightarrow X^2 \Sigma$) violet system, which
 163 might be generated through the reactions of excited N₂ molecules (or N atoms) with the methyl of
 164 toluene. Besides, in the plasma reforming of toluene (without H₂O, CO₂ or O₂), the deposition of non-
 165 volatile products with dark brown color can be observed on the electrodes and the reactor inner wall,
 166 which indicates that the formation of aromatic hydrocarbon agglomeration and soot in this reforming
 167 process [32].

168 Adding CO₂ into the N₂/C₇H₈ GA generates oxidative species such as O and OH radicals. For
 169 instance, the OH ($A^2 \Sigma^+ \rightarrow X^2 \Pi$) band was visible in the spectrum of the N₂/CO₂/C₇H₈ GA. Note
 170 steam was not introduced in this reaction, thus OH could be generated mainly through the reactions
 171 between toluene (or reaction intermediates) with O atoms from CO₂ decomposition (R4-R7)



176 Figure 3 shows the presence of CO₂ significantly decreases the relative intensity of CN. This
 177 finding suggests that the formation of CN might be associated with the reaction between nitrogen
 178 species and deposited carbon. In the plasma CO₂ reforming of toluene, the presence of CO₂ generates
 179 oxidative species such as OH and O radicals, which enhance the oxidation reaction and reduce carbon
 180 deposition, thus limiting the formation of CN.

181 In the N₂/H₂O/C₇H₈ GA, the NH ($A^2 \Sigma \rightarrow X^2 \Sigma$) transition was observed at 336.0 nm. Besides, the
 182 relative intensity of the OH band was much higher than that in the CO₂/N₂/C₇H₈ GA, indicating the
 183 dissociation of H₂O to OH by electrons and excited nitrogen species (R8 and R9) in the plasma steam

184 reforming of toluene.



187 The formation of NH might be associated with OH (R10) [33], as NH transition was not detected
188 in the spectrum of the N₂/C₇H₈ GA. This finding also suggests that NH might not be generated directly
189 through the reaction between N₂ and H₂ in this reaction.



191 When O₂ was introduced into the N₂/C₇H₈ GA the CO (*B*¹ Σ - *A*¹ Π) system at 200-240 nm, the NO _{λ}
192 bands in the range of 230-250 nm and the oxygen 777 nm triplet were detected (Figure 3). The
193 formation of O radicals might occur via the following reactions (R11 and R12):



196 Besides, the visible NO and CO bands in the N₂/O₂/C₇H₈ GA indicate that the reactions R13-R15
197 might take place.

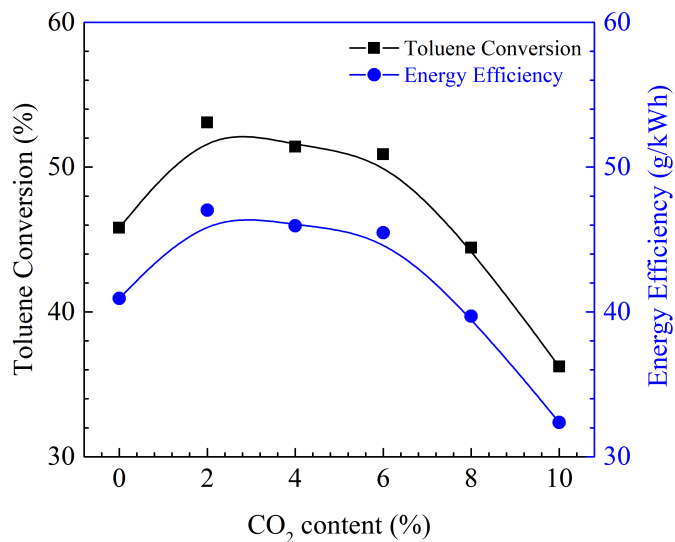


201

202 **3.2 Effect of CO₂ content**

203 Figure 4 shows the performance of the plasma reforming of toluene at different CO₂ contents.
204 Increasing the content of CO₂ initially enhanced the conversion of toluene and reached a peak (53.1%)
205 at a CO₂ content of 2 vol.%, beyond which the toluene conversion decreased to 36.2% when further

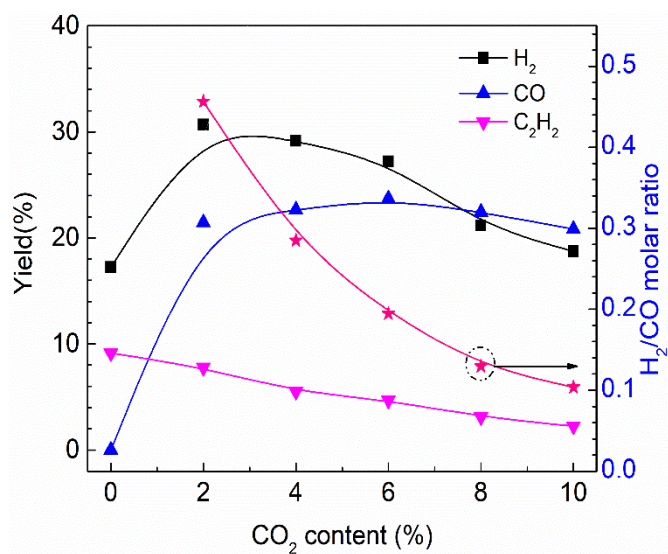
206 increasing the CO₂ content to 10 vol.%. In addition, the energy efficiency for toluene conversion in
207 the GA reactor followed the same pattern as the toluene conversion and reached a maximum value of
208 47.1 g/kWh at a CO₂ content of 2 vol.%.



209

210

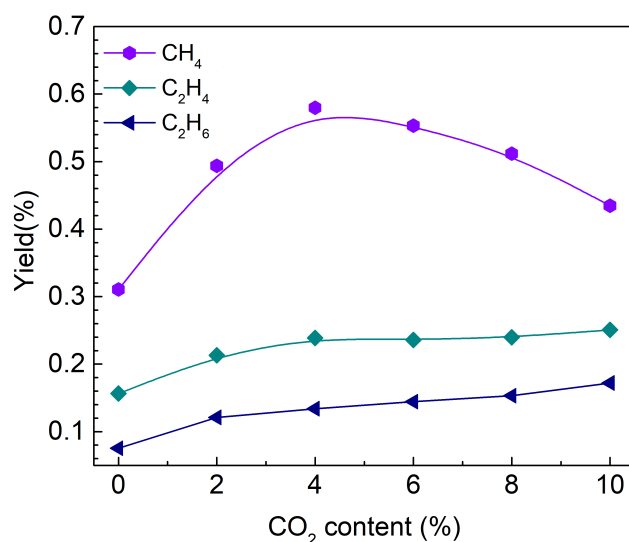
(a)



211

212

(b)



213

214

(c)

215

Figure 4. Effect of different CO₂ contents on the plasma reforming of toluene: (a) the conversion

216

of toluene and energy efficiency; (b) the yield of major gas products and H₂/CO molar ratio; (c)

217

the yield of minor gas products.

218

219

Previous studies reported that the initial conversion of toluene in an N₂ plasma is driven by either

220

electron impact dissociation or collisions with excited nitrogen species [34],

221



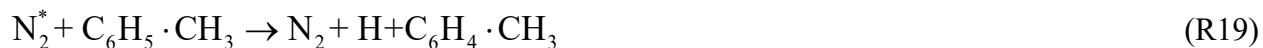
222



223



224



225



226

227

Adding CO₂ (2 vol.%) to the plasma reforming of toluene significantly improved the toluene

228

conversion, which can be mainly attributed to the enhanced oxidation of toluene and reaction

229

intermediates by generating more oxidative species such as O and OH radicals (R4 – R7). OH radicals

230 are more reactive in toluene oxidation compared to atomic O species. In the plasma CO₂ reforming
231 of toluene without steam, R6 was reported as the main route for the generation of OH radicals [35].
232 However, further increasing the CO₂ content decreased the toluene conversion, which might be
233 ascribed to the quenching of the populated excited nitrogen species and reduced number density of
234 energetic electrons by the presence of excessive CO₂. In addition, the excited N₂ species in the CO₂/N₂
235 mixture likely react with CO₂ instead of toluene, due to the relatively low dissociation energy of CO₂
236 (2.94 eV), which reduces the formation of excited nitrogen species and the chance for toluene to react
237 with these reactive species [36]. Meanwhile, the contribution of nitrogen excited species to the
238 conversion of toluene could be reduced due to the fast quenching of N₂ (A³) by CO (R21) [37]. Thus,
239 at a higher CO₂ content, the oxidation reactions are not sufficient to compensate for the decreased
240 toluene conversion due to the reduced fraction of nitrogen excited species and energetic electrons.
241 Similar results were also reported by Zhu and his co-workers [22].



243 Adding CO₂ to the plasma reforming of toluene significantly affects the distribution of the gas
244 products. In the plasma reforming of toluene without CO₂, H₂ and C₂H₂ were the major gas products
245 with a yield of 17.2% and 9.2%, respectively. However, increasing the CO₂ content to 10 vol.%
246 considerably decreased the yield of C₂H₂ by 76.0%. In contrast, the yield of CO increased to a
247 maximum of 23.7% in the plasma reforming of toluene containing 6 vol.% CO₂ and remained almost
248 stable when further rising the CO₂ concentration. In addition, the highest H₂/CO molar ratio (0.45)
249 was obtained at a CO₂ content of 2 vol.%, and this ratio decreased remarkably to 0.10 when increasing
250 the CO₂ content to 10 vol.% due to the formation of more CO. These findings suggest that adding an
251 appropriate amount of CO₂ favors the generation of syngas. Small amounts of CH₄, C₂H₄ and C₂H₆

252 with a yield of < 1% were also generated in this reaction, while no C₃ and C₄ hydrocarbons were
253 detected.

254

255 In the plasma CO₂ reforming of toluene, CO can be formed via CO₂ dissociation (R6 and R7) or
256 hydrogenation of CO₂ (R22). H₂ is formed via the recombination of two H atoms. In the plasma
257 reforming of toluene, the H atoms can be generated through the dehydrogenation of the methyl group
258 of toluene, as the C-H bonds in the methyl group show the weakest dissociation energy (3.7 eV) in
259 toluene [38]. The recombination of CH₃ radicals with H forms methane (R23). C₂H₄ and C₂H₆ can be
260 formed mainly through the reactions R24-R26. However, the yield of C₂H₄ and C₂H₆ was very limited
261 CO₂ reforming of toluene, suggesting these reactions might be negligible in this process. The
262 generation of an appreciable amount of acetylene in the nitrogen plasma reforming of toluene
263 indicates that the cleavage of the benzene ring of toluene occurs in the plasma conversion of toluene
264 (R27) [35]. Previous studies showed that nitrogen excited species play an important role in the ring
265 cleavage of aromatic hydrocarbons using non-thermal plasmas [39].

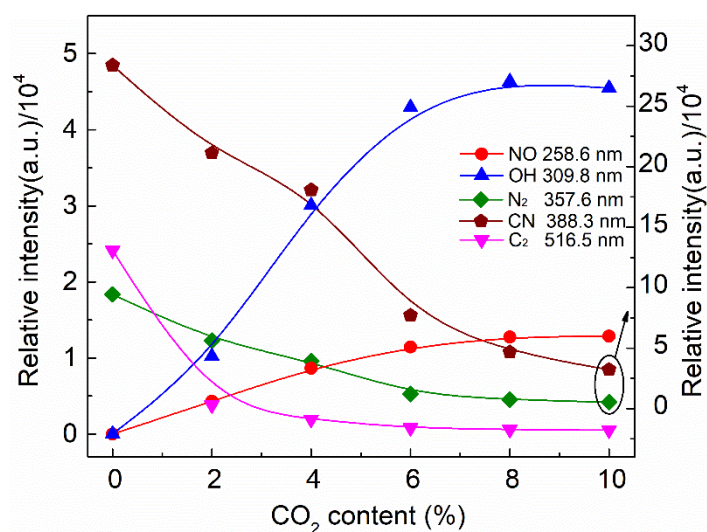


272

273 However, further increasing CO₂ content has a detrimental influence on the conversion of toluene

274 despite its importance for the generation of O and OH radicals to provide additional reaction routes
 275 for toluene conversion. Figure 5 shows the relative OES intensity of molecular bands in the plasma
 276 reforming of toluene with different CO₂ contents. Increasing the CO₂ content exponentially reduced
 277 the relative intensity of C₂ (516.5 nm) and N₂ band heads, which indicates that increasing the CO₂
 278 content consumes more electrons and limits the formation of nitrogen excited species.

279



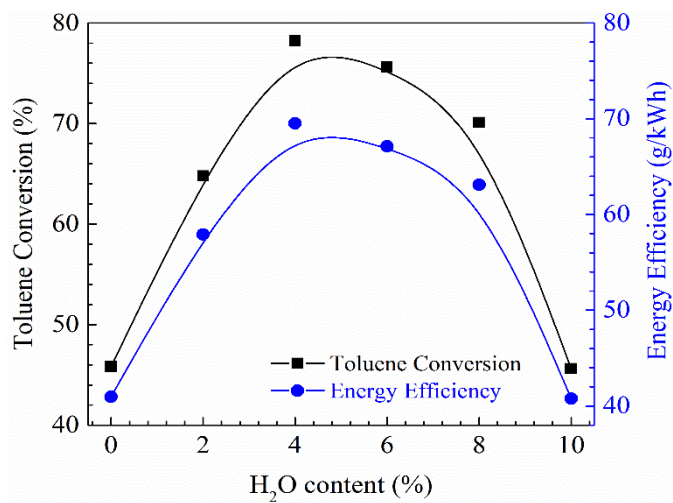
280

281 Figure 5. Effect of CO₂ content on the relative band head intensity in the plasma reforming of
 282 toluene.

283

284 3.3 Effect of steam content

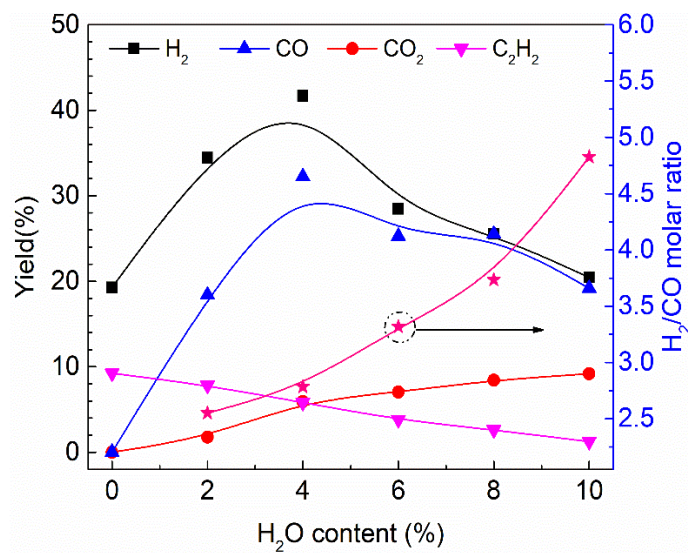
285 As shown in Figure 6 (a), the highest toluene conversion (78.3%) and energy efficiency (69.5
 286 g/kWh) can be achieved at the optimal H₂O content of 4 vol.%. Previous works also reported the
 287 presence of an optimal H₂O content or steam/carbon ratio to maximize the toluene conversion in
 288 plasma tar reforming processes [22, 40].



289

290

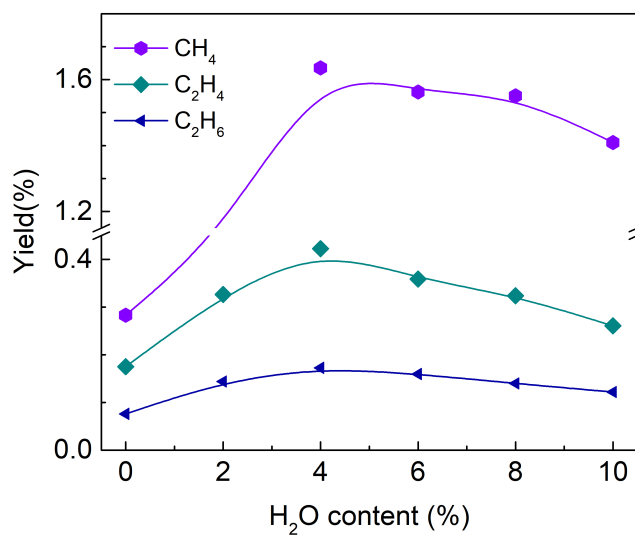
(a)



291

292

(b)



293

294

(c)

295

Figure 6. Effect of different steam contents on the plasma reforming of toluene: (a) the conversion

296

of toluene and energy efficiency; (b) the yield of major gas products and H₂/CO molar ratio; (c)

297

the yield of minor gas products.

298

299

Introducing steam into the discharge produces OH radicals through the dissociation of H₂O by

300

electrons (R8) and excited nitrogen species (R9). The OH radicals are more oxidative in toluene

301

conversion at low temperatures compared to atomic O species, as the reaction rate of toluene

302

oxidation with OH radicals is significantly higher than the oxidation of toluene with O radicals [34].

303

Figure 7 shows that increasing the content of H₂O from 0 to 4 vol.% significantly enhances the relative

304

intensity of the OH band head at 308.8 nm. Previous theoretical and experimental studies also

305

confirmed the oxidation of toluene by OH radicals through reactions R28-R29 [35].

306



307



308

309

However, increasing the content of H₂O from 4 to 10 vol.% considerably reduced the toluene

310

conversion. Due to the electronegativity of H₂O molecules, electrons can be consumed via electron

311

attachment (R30). At a lower H₂O content, the effect of electron attachment is insignificant, and the

312

presence of steam has a positive effect on the conversion of toluene resulted from the enhanced

313

oxidation of toluene and reaction intermediates induced by OH radicals. However, higher H₂O

314

contents (>4 vol.%) reduce the electron density due to the significant electron attachment with water,

315

while the presence of excessive water in the plasma also leads to the quenching of excited nitrogen

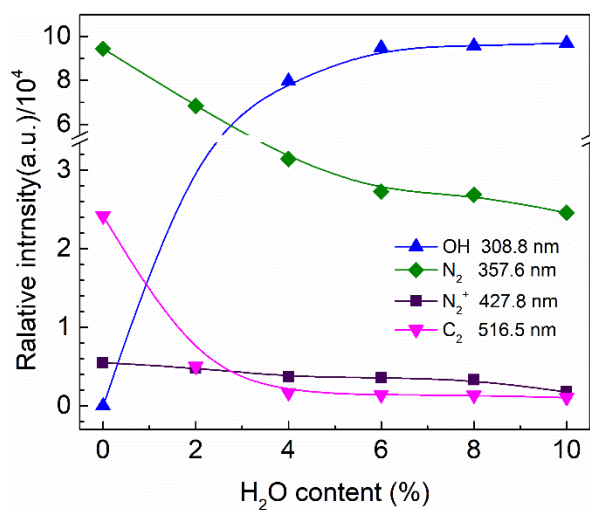
316 species. This hypothesis can be reflected by the OES analysis (Figure 7), showing that the relative
317 intensity of the OH band at 308.8 nm was almost unchanged when increasing the H₂O content from
318 6 vol.% to 10 vol.%. These opposite effects induced by the presence of higher H₂O contents lead to
319 the reduced toluene conversion in the plasma reforming process. Therefore, it is crucial to choose
320 appropriate steam content to maximize the conversion, syngas yield and energy efficiency in the
321 plasma reforming of tars.



323

324 The presence of steam not only influences the toluene conversion but also changes the distribution
325 of the gas products in the plasma reforming of toluene. As seen in Figure 6(b), increasing the content
326 of steam from 0 to 4 vol.% significantly increases the production of syngas, reaching the highest
327 syngas yield of 73.9% (41.7% for H₂ and 32.2% for CO) at an H₂O content of 4 vol.%; whereas
328 further increasing the H₂O content inhibited the generation of CO but enhanced the yield of CO₂ due
329 to the occurrence of the water-gas shift (WGS) reaction (R31). In contrast, the yield of C₂H₂ was
330 continuously decreased from 9.3% to 1.3% when increasing the H₂O content to 10 vol.% as oxidation
331 is more favourable compared to direct cleavage of benzene ring by excited nitrogen species and
332 electrons. This phenomenon can also be reflected by the decrease in the relative intensity of the C₂
333 band head (516.5 nm) when increasing the H₂O content.





335

336 Figure 7. Effect of H₂O content on the relative band head intensity in the plasma reforming of

337

toluene.

338

339 3.4 Effect of oxygen content

340 Figure 8 presents the effect of oxygen content on the plasma reforming of toluene. The presence of

341 oxygen is favorable for the conversion of toluene. Increasing the oxygen content from 0 to 10 vol.%

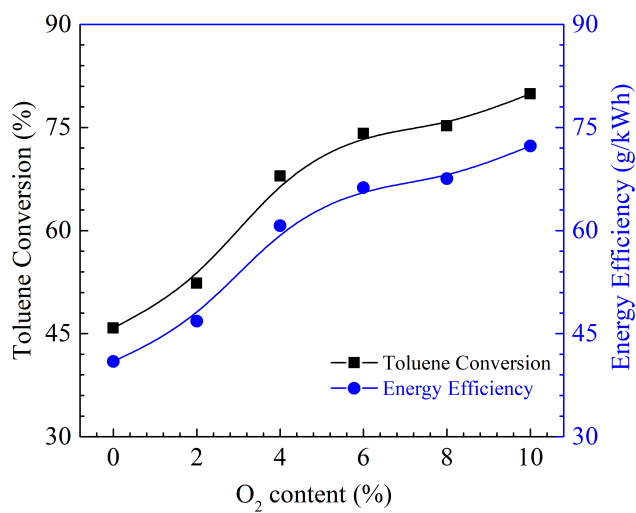
342 nearly doubled the toluene conversion and energy efficiency, which can be attributed to the enhanced

343 toluene oxidation due to the presence of more reactive O radicals in the plasma reaction containing

344 O₂ (R32 and R33), as shown in Figure 9. Similar findings were reported by Du and his coworkers

345 [41].

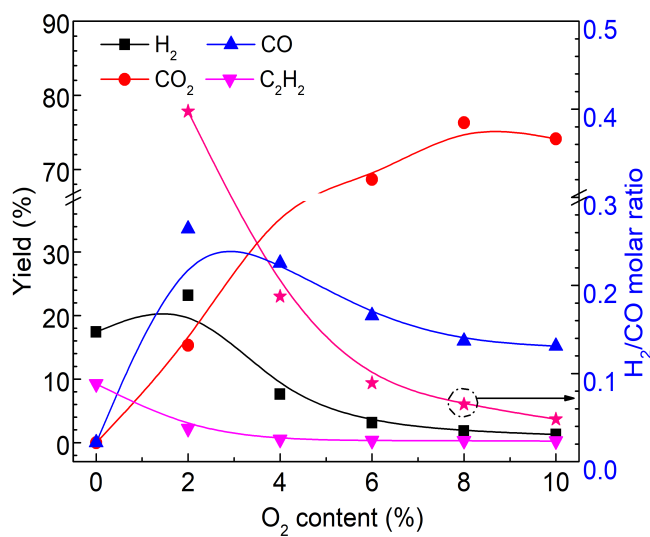




348

349

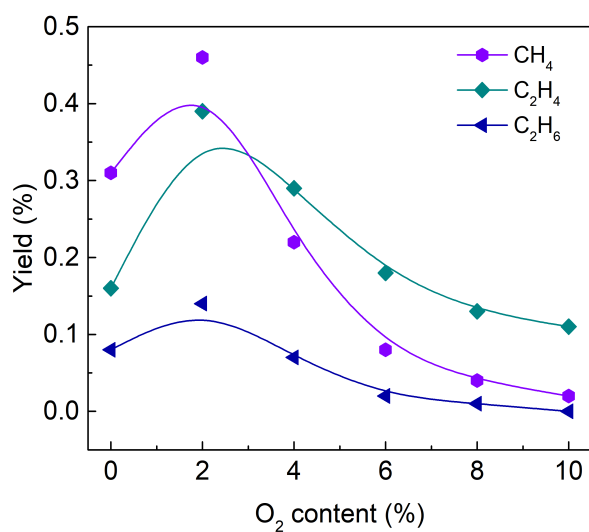
(a)



350

351

(b)



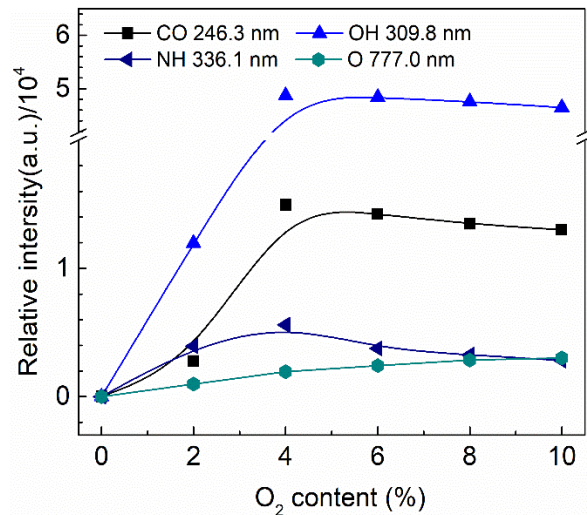
352

353

(c)

354 Figure 8. Effect of O₂ content on the plasma reforming of toluene: (a) the conversion of toluene
355 and energy efficiency; (b) the yield of major gas products and H₂/CO molar ratio; (c) the yield of
356 minor gas products.

357
358 The oxygen content also significantly influences the formation of gaseous products. Figure 8(b)
359 shows that the highest syngas yield is reached at a low oxygen content of 2 vol.%. Further increasing
360 the oxygen content to 10 vol.% gradually reduces the yield of H₂ and CO from 23.2% to 1.3% and
361 33.7% to 15.2%, respectively. At a lower oxygen content (≤ 2 vol.%), the highly reactive O
362 radicals produced through electron impact dissociation of O₂ promotes the conversion of
363 toluene to CO and H₂. However, a higher oxygen content (> 2 vol.%) can generate excessive O
364 radicals in the plasma reforming of toluene, inducing over-oxidation of toluene and reaction
365 intermediates and thus limiting the production of syngas by forming more CO₂ and H₂O. Note
366 the presence of O₂ also limited the yield of hydrocarbons ($< 0.5\%$), as shown in Figure 8(c).



367
368 Figure 9. Effect of O₂ content on the relative intensity of the molecular band heads (CO, NH and
369 OH) and O atomic line in the plasma reforming of toluene.

370

371 In the plasma reforming of toluene without oxidative gases (CO₂, H₂O and O₂), carbon deposition
372 can be found on the electrode surface and the inner wall of the GA reactor. In the presence of oxidative
373 gas (CO₂, H₂O or O₂), carbon deposition in the reactor was significantly reduced, resulted in a higher
374 carbon balance. In this study, the highest carbon balance of 67.9% was achieved in the plasma
375 reforming of toluene in the presence of 10 vol.% O₂. Additionally, we find that different oxidative
376 gases affect the toluene conversion, energy efficiency and syngas yield in the plasma reforming of
377 toluene in different ways. Increasing the content of O₂ improved the conversion of toluene and the
378 energy efficiency of the plasma reforming process. The highest toluene conversion (79.9%) and
379 energy efficiency (72.3 g/kWh) can be achieved simultaneously in the plasma reforming of toluene
380 with 10 vol.% O₂. However, the syngas yield was low in the presence of 10 vol.% O₂ due to over-
381 oxidation of toluene and reaction intermediates under these conditions. In the plasma reforming of
382 toluene using either CO₂ or steam, the optimal content of CO₂ and steam can be found to reach the
383 highest toluene conversion, syngas yield and energy efficiency simultaneously, suggesting that
384 appropriate content of CO₂ and steam is critical for the effective conversion of tars from biomass
385 gasification. In this work, the most promising performance was obtained when introducing steam to
386 the plasma reforming of toluene. A high toluene conversion of 78.3% was achieved with relatively
387 high energy efficiency (69.5 g/kWh) and a high syngas yield (73.9%) at the optimal steam content of
388 4 vol.%. Compared to the state-of-the-art in the plasma reforming of toluene using different plasma
389 technologies (e.g., microwave plasma, corona discharge, DBD and GA) [24], the energy efficiency
390 of toluene conversion in this work is much higher than that obtained using other types of plasma
391 reactors, indicating that GA is very promising for the conversion and re-utilization of biomass tars
392 with high efficiency.

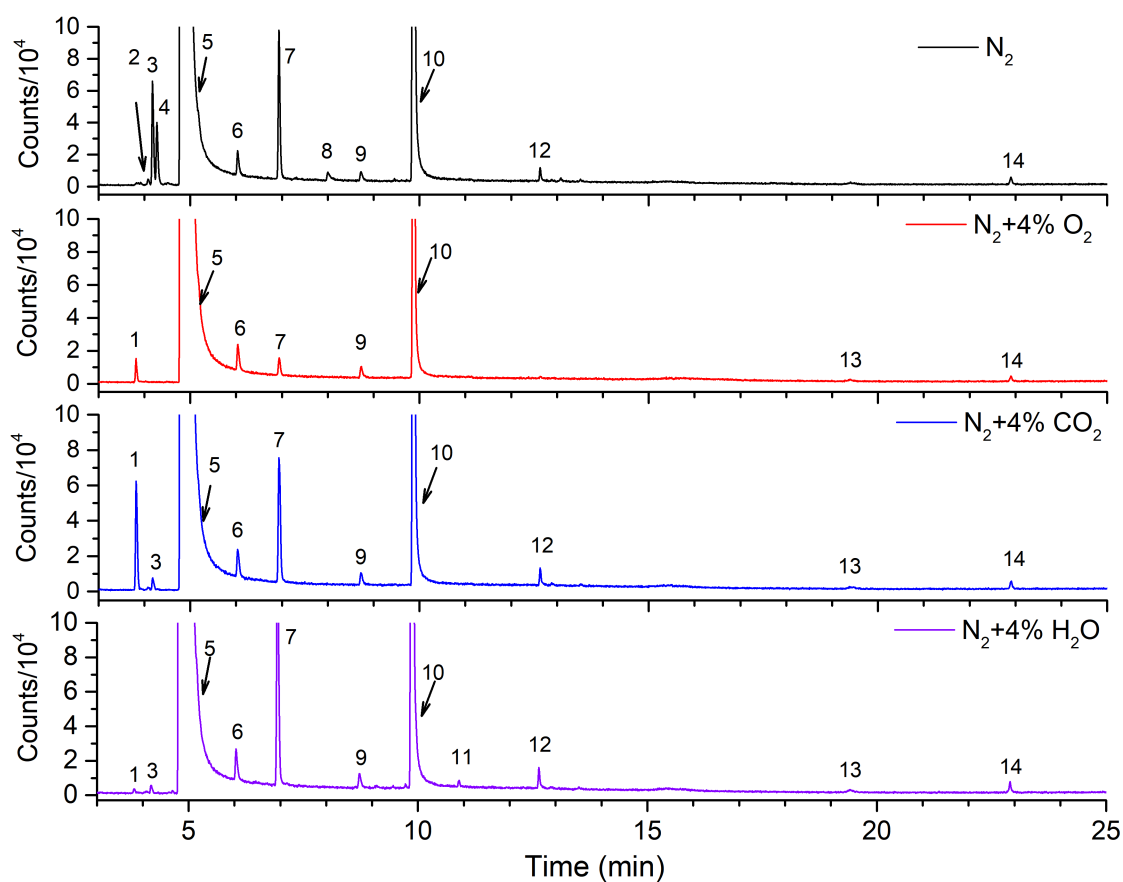
393

394 **3.5 Analysis of by-products**

395 To understand the reaction pathways in the plasma reforming of toluene, the collected liquid by-
396 products were analyzed using GC-MS, as shown in Figure 9. The corresponding structures of these
397 products are listed in Table 1. In the nitrogen plasma reforming of toluene without the oxidative gases,
398 nitrogen-containing compounds were detected in the collected liquids. The existence of
399 propionitrile compounds indicates that CN radicals contribute to the toluene conversion. The by-
400 products generated in the plasma reforming of toluene with oxidative gases (CO₂, O₂ and H₂O) were
401 different compared to the plasma reforming reaction without the oxidative gases. For instance,
402 oxygen-containing polycyclic aromatics were detected in the plasma reforming of toluene with
403 oxidative gases. The presence of oxygen-containing compounds, such as benzeneacetamide and
404 acetaldehyde suggests the occurrence of the reactions between the reaction intermediates and nitrogen
405 oxides. The compounds containing one-ring, such as ethylbenzene and 4-ethyltoluene could be
406 generated from the alkylation of benzene and toluene, respectively. The precursor of naphthalene
407 molecule indene was also detected, which reveals that the fragments of toluene recombine via radical
408 reactions to form high-molecular polymer compounds. The linear organic by-products, such as 1, 3-
409 butadiyne, 1-buten-3-yne and 3-methyl-1-butene might be generated by opening the toluene ring
410 followed by hydrogenation and/or oxidation of the resulting fragments. The presence of the aliphatic
411 compound, 2-Octene, indicates that the reactive C₂- and C₃-entities are easy to polymerize to
412 generate the linear hydrocarbons.

413 The formation of large molecules as by-products is not favourable in the plasma reforming of tars
414 and some of these by-products could be more toxic compared to the original tars [42]. For instance,

415 biphenyl is 2.5 times more toxic than benzene. Although it is difficult to quantify these liquid by-
 416 products, the concentration of these compounds could be several orders of magnitude lower than
 417 that of toluene (Figure 10), which indicates that the polymerization reactions have a minor
 418 contribution to the plasma reforming of toluene. It is important to control and reduce the formation
 419 of by-products in the plasma reforming of tars. The combination of plasma with catalysts has great
 420 potential to limit the formation of by-products for the selective production of clean syngas.



421
 422 Figure 10. GC-MS chromatograms of the collected liquids after the plasma toluene reforming (CO₂
 423 concentration: 4 vol.%; O₂ concentration: 4 vol.%; H₂O concentration: 4 vol.%).

424
 425 Table 1 Liquid compounds of the plasma reforming of toluene identified in Figure 10

No.	Time (min)	Chemical Name	Formula
-----	------------	---------------	---------


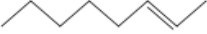
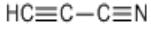

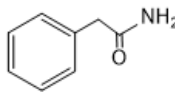

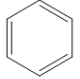
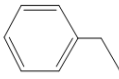
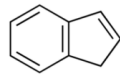
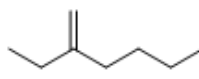
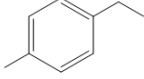
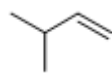
1	3.824	Acetaldehyde	C ₂ H ₄ O
2	4.087	1-Buten-3-yne	C ₄ H ₄
3	4.186	1,3-Butadiyne	C ₄ H ₂
4	4.281	Propiolonitrile	C ₃ HN
5	4.815	Dichloromethane	CH ₂ Cl ₂
6	6.039	3-Methyl-1-butene	C ₅ H ₁₀
7	6.938	Benzene	C ₆ H ₆
8	8.033	Heptane,3-methylene	C ₈ H ₁₆
9	8.721	2-Octene-(E)	C ₈ H ₁₆
10	9.871	Toluene	C ₇ H ₈
11	10.895	Benzeneacetamide	C ₈ H ₉ NO
12	12.63	Ethylbenzene	C ₈ H ₁₀
13	19.455	4-Ethyltoluene	C ₉ H ₁₂
14	22.904	Indene	C ₉ H ₈

426

427 Table 2 Effect of oxidative gases on the formation of liquid compounds in the plasma reforming of

428

toluene

General byproducts	Specific by-products					
	Background gas: N ₂		Background gas: N ₂ +H ₂ O, N ₂ +O ₂ , N ₂ +CO ₂			
						
1,3-Butadiyne	2-Octene-(E)	Propiolonitrile	1-Buten-3-yne	Benzeneacetamide	Acetaldehyde	
						
Benzene	Ethylbenzene	Indene	Heptane,3-methylene	4-Ethyltoluene	3-Methyl-1-butene	

429

430 4. Reaction mechanisms

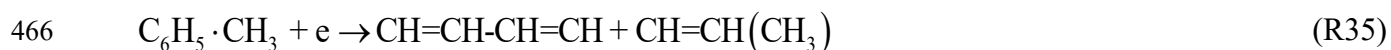
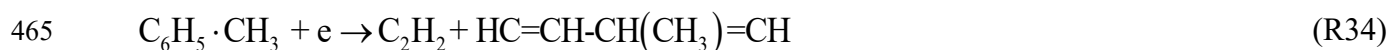
431 The identification of by-products in the plasma reforming of toluene using different carrier gases
432 indicates the existence of complex reaction pathways involving toluene molecules, carrier gases,
433 reactive species and intermediates. It is generally recognized that plasma toluene conversion can be
434 initiated through the dissociation of toluene and reaction intermediates by electrons, excited species
435 (e.g., nitrogen excited species in the presence of N₂ or air) and radicals (e.g., OH and O radicals) [43].
436 It is noteworthy that the concentration of toluene is significantly lower than that of the working gases
437 (nitrogen, carbon dioxide and H₂O molecules) in the plasma reforming of toluene. Thus, the energetic
438 electrons are more likely to collide with the carrier gas (nitrogen, carbon dioxide and H₂O molecules),
439 generating a range of reactive species, such as excited nitrogen species, O and OH radicals to initiate
440 chemical reactions[44]. Therefore, the electron impact dissociation of toluene is generally less
441 important compared to the direct dissociation of toluene by reactive species such as excited nitrogen
442 species and radicals.

443

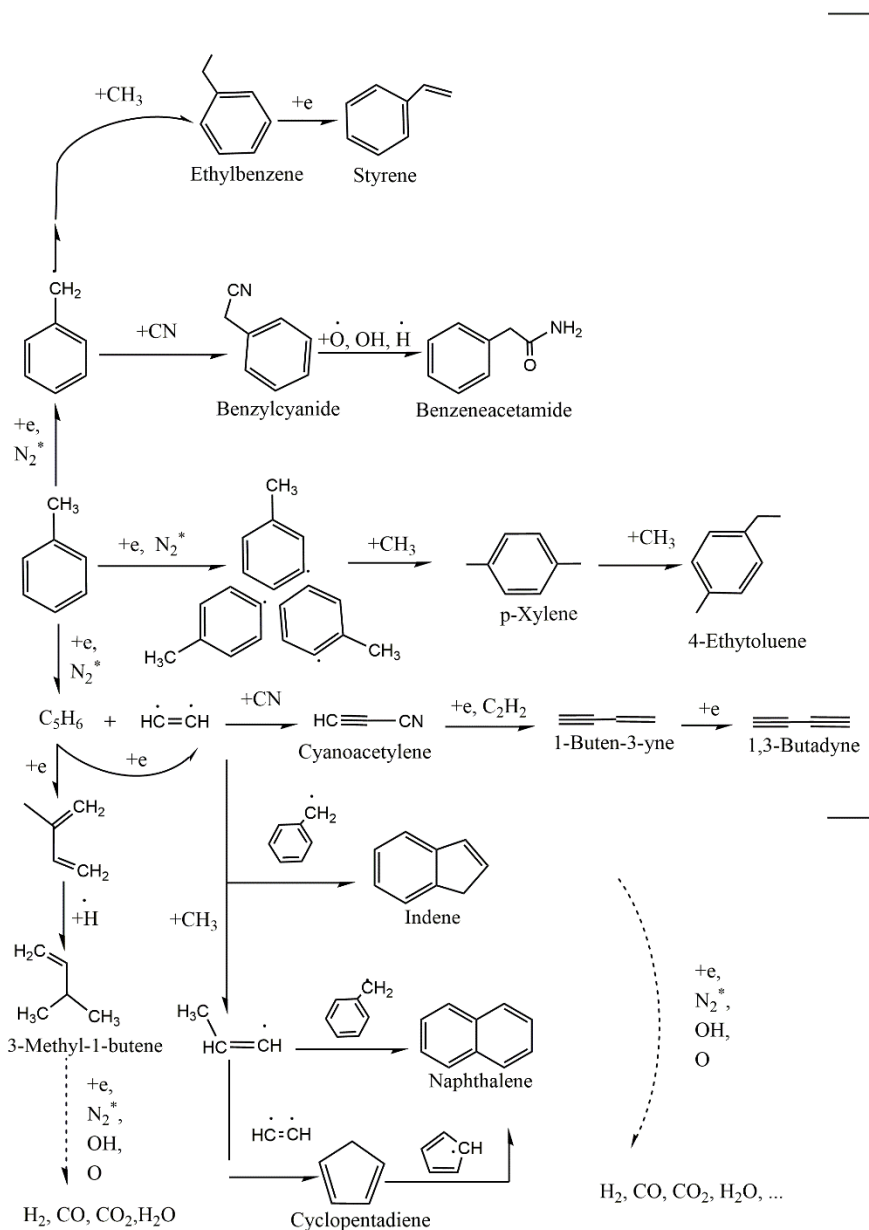
444 **4.1 Reaction pathways of toluene decomposition (I)**

445 The mean electron energy of a GA is generally between 1 and 3 eV [32]. In an N₂ or air plasma,
446 the excited nitrogen species can be generated through electron impact excitation of N₂. Figure 11
447 shows the proposed major reaction pathways initiated by excited nitrogen species and electrons in the
448 plasma reforming of toluene. The dissociation of toluene is initiated by energetic electrons and excited
449 nitrogen species, forming either aromatic radical cations or benzyl radicals [45]. The generated benzyl
450 radicals interact with methyl or CN radicals, forming ethylbenzene or benzyl-cyanide, respectively.
451 Afterwards, a step-wise dehydrogenation of ethylphenyl produces styrene [46]. The aromatic radical
452 cation, benzyl-cyanide can further react with reactive species such as O, OH or NH, resulting in the

453 formation of benzeneacetamide, as detected by GC-MS. Blin- Simiand et al. reported CN radicals
454 can react with phenyl or methyl-phenyl radicals in the plasma conversion of toluene [34]. Besides,
455 the aromatic radical cations can be formed through the dissociation of toluene by electrons and active
456 species (e.g., excited nitrogen species). However, the aromatic radical cations are unstable and can
457 be easily reacted with methyl to form xylenes. Under the plasma environment, the collision of
458 isomeric xylenes with energetic electrons and excited nitrogen species yields various aromatic
459 products, such as p-xylene and 4-ethyltoluene. Additionally, the C-C bond between the methyl group
460 and the aromatic group can be easily broken by electrons, generating a phenyl radical and a methyl
461 radical. The phenyl radical can react with atomic H to form benzene. Furthermore, energetic electrons
462 (over 5.5 eV) and nitrogen excited species can induce the direct cleavage of the aromatic ring,
463 resulting in the formation of ring-opening products (e.g., acetylene and C₅H₆). Liang et al. reported
464 the possible ring-open reactions for the conversion of toluene, as shown in R34 and R35 [47].



467 The generated aromatic intermediates can be further dissociated by the energetic electrons and
468 excited nitrogen species, resulting in the rupture of aromatic rings. The partially decomposed species
469 can further react with electrons and active species, generating the final products (H₂O, CO and CO₂).



470

471 Figure 11. Major reaction pathways initiated by energetic electrons and excited N₂ species in the
 472 plasma reforming of toluene.

473

474 In addition to the aforementioned proposed reaction pathways, the plasma conversion of toluene is
 475 also associated with the formation of polycyclic aromatic compounds, mainly 2-ring compounds. In
 476 this study, indene, a precursor of naphthalene was identified as a trace by-product in the plasma
 477 reforming with or without the oxidative gases, which indicates that indene may be generated by a

478 direct combination of aromatic rings. Previous work reported that the recombination of aromatic rings
479 contributes to the formation of polycyclic compounds in the plasma conversion of benzene or toluene
480 [42, 48]. The formation of indene can be induced by the H-abstraction of toluene to generate benzyl
481 followed by the acetylene addition and hydrogenation, which leads to molecular growth by
482 cyclisation. Similarly, the cyclopentadienyl radicals are mainly generated by the recombination of
483 acetylene and propyne, while the cyclopentadienyl radicals are mainly formed by the recombination
484 of allyl radicals and acetylene. The recombination of two cyclopentadienyl radicals forms
485 naphthalene [49].

486

487 **4.2 Reaction pathways of toluene decomposition (II)**

488 In the plasma reforming of toluene using the oxidative gases (CO_2 , H_2O and O_2), the conversion
489 of toluene and reaction intermediates can proceed through step-wise oxidation by oxidative species
490 such as O and OH radicals generated in the plasma. However, these oxidation pathways are only
491 significant when an appropriate content of H_2O , CO_2 or O_2 is present in the plasma toluene reforming
492 process. For example, the presence of higher H_2O contents in the plasma reforming of toluene reduces
493 the electron density due to electron attachment with water, and consequently reduces the conversion
494 of toluene. As OH radicals are more oxidative than atomic O species, the contribution of OH radicals
495 to the conversion of toluene could be more significant even the concentration of OH radicals is lower
496 than that of O atoms in the plasma reforming process. Durme et al. found that the first step in toluene
497 oxidation is either the abstraction of a hydrogen atom from the methyl group of toluene by OH to
498 generate benzyl alcohol; or the addition of an OH radical to the aromatic ring of toluene to form
499 $\text{C}_6\text{H}_5\text{OHCH}_3$ or cresol [48]. Benzyl alcohol can be further oxidized to benzaldehyde and then

500 transferred to benzoic acid, which then generates benzene and CO₂ via the photo-kolbe reaction.

501 Additionally, the structure of the intermediate C₆H₅OHCH₃ is unstable and can be transformed to

502 oxygen-enriched peroxide radicals C₆H₅OHOOCH₃ by rapidly opening the aromatic ring. Then,

503 C₆H₅OHOOCH₃ reacts with oxygen species or OH radicals through H-abstraction to form carbonyl

504 derivative, notably aldehydes. After that, the ring-cleavage aromatic compounds may be further

505 fragmented to generate the hydroxylated intermediates, which are gradually mineralized into the final

506 products (CO and CO₂). Previous experimental results implied that aldehydes are the common

507 products in the plasma oxidation of aromatic compounds, for instance, HCHO and CH₃CHO were

508 detected as the major by-products in the plasma destruction of toluene in the humid environment [50].

509 Our measurements demonstrated the formation of some carbonyl derivatives, notably acetaldehyde

510 and benzeneacetamide in the plasma reforming of toluene with either O₂ or steam; however,

511 carboxylic acid was not detected. This finding suggests that the generated HCHO could be fully

512 oxidized to H₂O and CO₂ in the presence of O and OH radicals in the plasma reforming of toluene.

513 Previous studies confirmed that the oxidative reaction pathways significantly contribute to the

514 conversion of toluene in the plasma processing of toluene with oxidative gases [35]. Figure 12

515 presents the possible pathways in the conversion of toluene by oxidative species.

524 in the plasma reforming of toluene through the creation of new reaction pathways. Adding a low
525 concentration of CO₂ (2 vol.%) in the plasma reaction enhanced the conversion of toluene, whereas
526 further increasing the CO₂ content (2 - 10 vol.%) substantially reduced the conversion of toluene. The
527 presence of H₂O in the plasma process produces OH radicals which enhances the oxidation of toluene.
528 However, introducing excessive H₂O to the plasma reforming negatively affected the conversion of
529 toluene due to the electron attachment of H₂O molecules. The optimum H₂O content of 4 vol.% was
530 found to achieve the highest toluene conversion, syngas yield and energy efficiency simultaneously
531 in the plasma reforming of toluene. The presence of oxygen in the plasma tar reforming was favorable
532 for the conversion of toluene but significantly inhibited the formation of syngas alongside the
533 production of more CO₂. In this study, the highest toluene conversion (78.3%), energy efficiency
534 (69.5 g/kWh) and syngas yield (73.9%) were achieved in the plasma steam reforming of toluene
535 containing 4 vol.% H₂O. The combination of optical emission spectroscopic diagnostics and
536 gas/liquid analysis enables us to propose the possible major reaction pathways in the plasma
537 reforming of toluene. The initial dissociation of toluene is mainly induced by energetic electrons,
538 excited nitrogen species and oxidative species (e.g., O and OH radicals). The predominance of these
539 reactions in the plasma reforming of toluene is dependent on the content of oxidative gases. In the
540 presence of an optimal content of the oxidative gas (CO₂, steam and O₂), the oxidation reactions play
541 a significant role in the conversion of toluene and reaction intermediates.

542

543 **Acknowledgements**

544 The support of this work by the National Natural Science Foundation of China (No.51907087), the
545 Natural Science Foundation of Jiangsu Province (No. BK20190675), High-level Innovation and

546 Entrepreneurship Talents Introduction Program of Jiangsu Province, the Postdoctoral Science
547 Foundation (No. 2020M671289) are gratefully acknowledged. Y. Ma and X. Tu acknowledge the
548 funding from the Royal Society Newton Advanced Fellowship (NAF/R1180230) and British Council
549 (No. 623389161) .

550 **References**

- 551 [1] J. Ren, Y.-L. Liu, X.-Y. Zhao, J.-P. Cao, Biomass thermochemical conversion: A review on tar elimination from
552 biomass catalytic gasification, *Journal of the Energy Institute*, 93 (2020) 1083-1098.
- 553 [2] Y. Shen, K. Yoshikawa, Recent progresses in catalytic tar elimination during biomass gasification or pyrolysis—A
554 review, *Renewable and Sustainable Energy Reviews*, 21 (2013) 371-392.
- 555 [3] A. Bogaerts, X. Tu, J.C. Whitehead, G. Centi, L. Lefferts, O. Guaitella, F. Azzolina-Jury, H.-H. Kim, A.B. Murphy,
556 W.F. Schneider, T. Nozaki, J.C. Hicks, A. Rousseau, F. Thevenet, A. Khacef, M. Carreon, The 2020 plasma catalysis
557 roadmap, *Journal of Physics D: Applied Physics*, 53 (2020) 443001.
- 558 [4] D. Mei, X. Zhu, C. Wu, B. Ashford, P.T. Williams, X. Tu, Plasma-photocatalytic conversion of CO₂ at low
559 temperatures: Understanding the synergistic effect of plasma-catalysis, *Applied Catalysis B: Environmental*, 182 (2016)
560 525-532.
- 561 [5] B. Huang, C. Zhang, H. Bai, S. Zhang, K. Ostrikov, T. Shao, Energy pooling mechanism for catalyst-free methane
562 activation in nanosecond pulsed non-thermal plasmas, *Chemical Engineering Journal*, 396 (2020) 125185.
- 563 [6] A. George, B. Shen, M. Craven, Y. Wang, D. Kang, C. Wu, X. Tu, A review of non-thermal plasma technology: A
564 novel solution for CO₂ conversion and utilization, *Renewable and Sustainable Energy Reviews*, 135 (2021) 109702.
- 565 [7] D.H. Mei, X.B. Zhu, Y.L. He, J.D. Yan, X. Tu, Plasma-assisted conversion of CO₂ in a dielectric barrier discharge
566 reactor: understanding the effect of packing materials, *Plasma Sources Science & Technology*, 24 (2015).
- 567 [8] R. Zhou, R. Zhou, Y. Xian, Z. Fang, X. Lu, K. Bazaka, A. Bogaerts, K. Ostrikov, Plasma-enabled catalyst-free
568 conversion of ethanol to hydrogen gas and carbon dots near room temperature, *Chemical Engineering Journal*, 382 (2020)
569 122745.
- 570 [9] R. Zhou, R. Zhou, S. Wang, U.G. Mihiri Ekanayake, Z. Fang, P.J. Cullen, K. Bazaka, K.K. Ostrikov, Power-to-
571 chemicals: Low-temperature plasma for lignin depolymerisation in ethanol, *Bioresource technology*, (2020) 123917.
- 572 [10] D. Mei, S. Liu, S. Wang, R. Zhou, R. Zhou, Z. Fang, X. Zhang, P.J. Cullen, K. Ostrikov, Plasma-enabled liquefaction
573 of lignocellulosic biomass: Balancing feedstock content for maximum energy yield, *Renewable Energy*, 157 (2020) 1061-
574 1071.
- 575 [11] P. Chawdhury, D. Ray, C. Subrahmanyam, Single step conversion of methane to methanol assisted by nonthermal
576 plasma, *Fuel Processing Technology*, 179 (2018) 32-41.
- 577 [12] D.B. Nguyen, S. Shirjana, M.M. Hossain, I. Heo, Y.S. Mok, Effective generation of atmospheric pressure plasma in
578 a sandwich-type honeycomb monolith reactor by humidity control, *Chemical Engineering Journal*, 401 (2020) 125970.
- 579 [13] E. Blanquet, M.A. Nahil, P.T. Williams, Enhanced hydrogen-rich gas production from waste biomass using pyrolysis
580 with non-thermal plasma-catalysis, *Catalysis Today*, 337 (2019) 216-224.
- 581 [14] P. Chawdhury, Y. Wang, D. Ray, S. Mathieu, N. Wang, J. Harding, F. Bin, X. Tu, C. Subrahmanyam, A promising
582 plasma-catalytic approach towards single-step methane conversion to oxygenates at room temperature, *Applied Catalysis*
583 *B: Environmental*, 284 (2021).
- 584 [15] H. Zhang, X. Li, F. Zhu, K. Cen, C. Du, X. Tu, Plasma assisted dry reforming of methanol for clean syngas production
585 and high-efficiency CO₂ conversion, *Chemical Engineering Journal*, 310 (2017) 114-119.
- 586 [16] L. Wang, Y. Yi, H. Guo, X. Tu, Atmospheric pressure and room temperature synthesis of methanol through plasma-
587 catalytic hydrogenation of CO₂, *ACS Catalysis*, 8 (2018) 90-100.
- 588 [17] S.A. Nair, A.J.M. Pemen, K. Yan, F.M. van Gompel, H.E.M. van Leuken, E.J.M. van Heesch, K.J. Ptasinski, A.A.H.
589 Drinkenburg, Tar removal from biomass-derived fuel gas by pulsed corona discharges, *Fuel Processing Technology*, 84
590 (2003) 161-173.
- 591 [18] Y. Sekine, K. Urasaki, S. Kado, M. Matsukata, E. Kikuchi, Nonequilibrium pulsed discharge: A novel method for
592 steam reforming of hydrocarbons or alcohols, *Energy & Fuels*, 18 (2004) 455-459.

593 [19] S.Y. Liu, D.H. Mei, M.A. Nahil, S. Gadkari, S. Gu, P.T. Williams, X. Tu, Hybrid plasma-catalytic steam reforming
594 of toluene as a biomass tar model compound over Ni/Al₂O₃ catalysts, *Fuel Processing Technology*, 166 (2017) 269-275.

595 [20] B. Xu, N. Wang, J. Xie, Y. Song, Y. Huang, W. Yang, X. Yin, C. Wu, Removal of toluene as a biomass tar surrogate
596 by combining catalysis with nonthermal plasma: understanding the processing stability of plasma catalysis, *Catalysis
597 Science & Technology*, 10 (2020) 6953-6969.

598 [21] L. Liu, Y. Liu, J. Song, S. Ahmad, J. Liang, Y. Sun, Plasma-enhanced steam reforming of different model tar
599 compounds over Ni-based fusion catalysts, *Journal of Hazardous Materials*, 377 (2019) 24-33.

600 [22] F. Zhu, H. Zhang, H. Yang, J. Yan, X. Li, X. Tu, Plasma reforming of tar model compound in a rotating gliding arc
601 reactor: Understanding the effects of CO₂ and H₂O addition, *Fuel*, 259 (2020).

602 [23] H. Zhang, F. Zhu, X. Li, R. Xu, L. Li, J. Yan, X. Tu, Steam reforming of toluene and naphthalene as tar surrogate in
603 a gliding arc discharge reactor, *Journal of Hazardous Materials*, 369 (2019) 244-253.

604 [24] D. Mei, Y. Wang, S. Liu, M. Alliat, H. Yang, X. Tu, Plasma reforming of biomass gasification tars using mixed
605 naphthalene and toluene as model compounds, *Energy Conversion and Management*, 195 (2019) 409-419.

606 [25] D. Mei, S. Liu, Y. Wang, H. Yang, Z. Bo, X. Tu, Enhanced reforming of mixed biomass tar model compounds using
607 a hybrid gliding arc plasma catalytic process, *Catalysis Today*, 337 (2019) 225-233.

608 [26] Y. Wang, H. Yang, X. Tu, Plasma reforming of naphthalene as a tar model compound of biomass gasification, *Energy
609 Conversion and Management*, 187 (2019) 593-604.

610 [27] M. Mlotek, J. Woroszyl, B. Ulejczyk, K. Krawczyk, Coupled plasma-catalytic system with rang 19pr catalyst for
611 conversion of tar, *Scientific Reports*, 9 (2019) 13562.

612 [28] Y. Wang, Z. Liao, S. Mathieu, F. Bin, X. Tu, Prediction and evaluation of plasma arc reforming of naphthalene using
613 a hybrid machine learning model, *Journal of Hazardous Materials*, 404 (2021) 123965.

614 [29] M.L. Valderrama Rios, A.M. González, E.E.S. Lora, O.A. Almazán del Olmo, Reduction of tar generated during
615 biomass gasification: A review, *Biomass and Bioenergy*, 108 (2018) 345-370.

616 [30] X. Tu, J.C. Whitehead, Plasma dry reforming of methane in an atmospheric pressure AC gliding arc discharge: Co-
617 generation of syngas and carbon nanomaterials, *International Journal of Hydrogen Energy*, 39 (2014) 9658-9669.

618 [31] M. Kong, Q. Yang, J. Fei, X. Zheng, Experimental study of Ni/MgO catalyst in carbon dioxide reforming of toluene,
619 a model compound of tar from biomass gasification, *International Journal of Hydrogen Energy*, 37 (2012) 13355-13364.

620 [32] L. Yu, X. Tu, X. Li, Y. Wang, Y. Chi, J. Yan, Destruction of acenaphthene, fluorene, anthracene and pyrene by a dc
621 gliding arc plasma reactor, *Journal of Hazardous Materials*, 180 (2010) 449-455.

622 [33] H. Zhang, F. Zhu, X. Li, K. Cen, C. Du, X. Tu, Rotating gliding arc assisted water splitting in atmospheric nitrogen,
623 *Plasma Chemistry and Plasma Processing*, 36 (2016) 813-834.

624 [34] N. Blin-Simiand, F. Jorand, L. Magne, S. Pasquiers, C. Postel, J.R. Vacher, Plasma reactivity and plasma-surface
625 interactions during treatment of toluene by a dielectric barrier discharge, *Plasma Chemistry and Plasma Processing*, 28
626 (2008) 429-466.

627 [35] A.N. Trushkin, I.V. Kochetov, Simulation of toluene decomposition in a pulse-periodic discharge operating in a
628 mixture of molecular nitrogen and oxygen, *Plasma Physics Reports*, 38 (2012) 407-431.

629 [36] M.A. Lindon, E.E. Scime, CO₂ dissociation using the Versatile atmospheric dielectric barrier discharge experiment
630 (VADER), *Frontiers in Physics*, 2 (2014).

631 [37] V.A. Bityurin, E.A. Filimonova, G.V. Naidis, Simulation of naphthalene conversion in biogas initiated by pulsed
632 corona discharges, *IEEE Transactions on Plasma Science*, 37 (2009) 911-919.

633 [38] F.S. Zhu, X.D. Li, H. Zhang, A.J. Wu, J.H. Yan, M.J. Ni, H.W. Zhang, A. Buckens, Destruction of toluene by rotating
634 gliding arc discharge, *Fuel*, 176 (2016) 78-85.

635 [39] Z. Machala, M. Morvová, E. Marode, I. Morva, Removal of cyclohexanone in transition electric discharges at
636 atmospheric pressure, *Journal of Physics D: Applied Physics*, 33 (2000) 3198-3213.

637 [40] L. Liu, Z. Zhang, S. Das, S. Kawi, Reforming of tar from biomass gasification in a hybrid catalysis-plasma system:
638 A review, *Applied Catalysis B: Environmental*, 250 (2019) 250-272.

639 [41] C.M. Du, J.H. Yan, B. Cheron, Decomposition of toluene in a gliding arc discharge plasma reactor, *Plasma Sources
640 Science & Technology*, 16 (2007) 791-797.

641 [42] S. Lee, S.-J. Liu, OES and GC/MS study of RF plasma of xylenes, *Plasma Chemistry and Plasma Processing*, 37
642 (2016) 149-158.

643 [43] H. Huang, D. Ye, D.Y.C. Leung, F. Feng, X. Guan, Byproducts and pathways of toluene destruction via plasma-
644 catalysis, *Journal of Molecular Catalysis a-Chemical*, 336 (2011) 87-93.

645 [44] A.A. Abdelaziz, T. Seto, M. Abdel-Salam, Y. Otani, Performance of a surface dielectric barrier discharge based
646 reactor for destruction of naphthalene in an air stream, *Journal of Physics D: Applied Physics*, 45 (2012) 115201.

647 [45] S. Liu, D. Mei, L. Wang, X. Tu, Steam reforming of toluene as biomass tar model compound in a gliding arc discharge
648 reactor, *Chemical Engineering Journal*, 307 (2017) 793-802.

649 [46] M. Sleiman, P. Conchon, C. Ferronato, J.-M. Chovelon, Photocatalytic oxidation of toluene at indoor air levels (ppbv):
650 Towards a better assessment of conversion, reaction intermediates and mineralization, *Applied Catalysis B:
651 Environmental*, 86 (2009) 159-165.

652 [47] W. Liang, J. Li, J. Li, Y. Jin, Abatement of toluene from gas streams via ferro-electric packed bed dielectric barrier
653 discharge plasma, *Journal of hazardous materials*, 170 (2009) 633-638.

654 [48] J. Van Durme, J. Dewulf, W. Sysmans, C. Leys, H. Van Langenhove, Abatement and degradation pathways of toluene
655 in indoor air by positive corona discharge, *Chemosphere*, 68 (2007) 1821-1829.

656 [49] K. Norinaga, H. Yang, R. Tanaka, S. Appari, K. Iwanaga, Y. Takashima, S. Kudo, T. Shoji, J.-i. Hayashi, A
657 mechanistic study on the reaction pathways leading to benzene and naphthalene in cellulose vapor phase cracking,
658 *Biomass and Bioenergy*, 69 (2014) 144-154.

659 [50] H.M. Lee, Abatement of Gas-phase p-Xylene via Dielectric Barrier Discharges, *Plasma Chemistry and Plasma
660 Processing*, 23 (2003) 541-558.

661
662